BPB Reports

Regular Article

Phosphorylation Dynamics and Kinase Interaction in mRNA Transcription-Associated Kinases: Autophosphorylation of CDK12 and its Modulation by CDK7 and CDK9

Hiroko Yamakawa,[a,b] Shunsuke Ebara,[a,b] Misaki Yoshida,[b] Koji Yamamoto,[c] Kozo Hayashi,[d] Kenichiro Shimokawa,[b] Shinsuke Araki,[e] Hiroshi Tauchi,[a,*] and Daisuke Morishita[b,*]

[a]*Department of Biological Sciences, Faculty of Science, Ibaraki University, 2-1-1 Bunkyo, Mito, Ibaraki 310-8512, Japan;* [b]*Chordia Therapeutics Inc., 2-26-1, Muraoka-Higashi, Fujisawa, Kanagawa, 251-0012, Japan;* [c]*Metcoding, 6-10-2 Kenkyu-Gakuen, Tsukuba, Ibaraki, 305-0817, Japan;* [d]*Axcelead Drug Discovery Partners, 2-26-1, Muraoka-Higashi, Fujisawa, Kanagawa, 251-0012, Japan;* [e]*Takeda Pharmaceutical Company, 2-26-1, Muraoka-Higashi, Fujisawa, Kanagawa, 251-0012, Japan*

Received August 20, 2024; Accepted August 29, 2024

Transcription of mRNA consists of three critical steps - initiation, elongation, and termination - and is driven by RNA polymerase II (Pol II), whose activity is regulated by a unique C-terminal domain (CTD). The transcription-related kinases CDK7, CDK9, and CDK12 regulate transcription by differentially phosphorylating serine 2, serine 5, and serine 7 of the Pol II CTD, although their functional interactions are not yet fully understood. Since these CDKs are involved in cancer cell proliferation and survival, elucidating these interactions is useful for cancer treatment. We focused on CDK12, which plays an important role in the late phase of transcription and identified several novel autophosphorylation sites of CDK12. Among these, serine 423 on CDK12 was found to be a critical residue affecting the half-life of the CDK12 protein and its phosphorylation is mediated by both CDK12 and CDK7. Additionally, comprehensive phosphoproteomic analysis revealed that CDK7 and CDK9 affect the phosphorylation of CDK12 and the CDK12 interactome, suggesting crosstalk between these kinases. Inhibition of CDK7 disrupted the interaction between CDK12 and proteins phosphorylated by CDK12, including RNA processing factors, while inhibition of CDK7 and CDK9 enhanced the interaction between CDK12 and splicing factors. In conclusion, our results indicate that CDK7 and CDK9 functionally regulate CDK12 upstream, suggesting that transcriptional CDKs cooperatively regulate RNA transcription and subsequent transcriptional processes.

Key words mRNA transcription, autophosphorylation, transcription-associated kinases, CDK7, CDK9, CDK12

INTRODUCTION

mRNA transcription is a fundamental process within the central dogma, which produce mRNA that serves as a template for protein synthesis. Given its crucial role in determining protein levels, this process demands tight and precise regulation. Transcription is carried out by RNA polymerase II (Pol II), which comprises several protein subunits. Among these subunits, the C-terminal domain (CTD) plays an indispensable role in the transcriptional activity of Pol II.[1)] Proper phosphorylation of the CTD, mediated by transcription-associated kinases, specifically cyclin-dependent kinases (CDKs), is essential for its function. Specifically, CDK7 promotes initiation by phosphorylating Ser7 and Ser5, while CDK9 and CDK12 enhance early-stage elongation and late-stage termination by cooperatively phosphorylating Ser2.[2)]

Although the molecular interactions between each CDK and the CTD have been well-studied, the interplay among these CDKs themselves has not been thoroughly investigated. Recent observations suggest such interactions exist: CDK7 phosphorylates key amino acid residues of CDK9 and CDK12, and CDK12 phosphorylates residues of CDK9.[3,4)] However, comprehensive phosphoproteomics analyses on CDK12 affected by CDK7 or CDK9 have not yet been conducted.

In this study, we aimed to identify the autophosphorylation sites of CDK12. Following this site identification, we evaluated the effects of CDK7 or CDK9 inhibition on autophosphorylation sites of CDK12 using phosphoproteomics methods. Additionally, we examined the influence of CDK7 or CDK9 inhibition on the CDK12 interactome. Based on these investigations, we finally explored the biological impact of the identified CDK12's phosphorylation sites on the CDK12 protein function.

*To whom correspondence should be addressed. e-mail: daisuke.morishita@chordiatherapeutics.com; daisuke.morishita.phd@gmail.com hiroshi.tauchi.sci@vc.ibaraki.ac.jp

MATERIAL AND METHODS

Reagents and Cell Culture CDK7 inhibitor CT7001 (Samuraciclib) and CDK9 inhibitor BAY-1251152 (Enitociclib) were purchased from MedChemExpress. Cycloheximide was obtained from Fujifilm Wako Pure Chemical. The CDK12 inhibitor (CDK12i) used for phosphoproteomics was synthesized by Takeda (WO2019/189555). Kinase selectivity for CDK12i was evaluated using previously described methods.[5] Human embryonic kidney 293T cells (ATCC) were cultured in Dulbecco's Modified Eagle's Medium (DMEM) supplemented with 10% fetal bovine serum (FBS). Breast inflammatory carcinoma SUM149PT cells (BioIVT) were cultured in Ham's F-12 medium supplemented with 5% FBS, 10 mM HEPES, 1 μg/mL hydrocortisone, and 5 μg/mL insulin. Human ovarian carcinoma A2780 cells (CancerTools) were cultured in Roswell Park Memorial Institute (RPMI) 1640 medium supplemented with 10% FBS. The CellTiter-Glo assay (Promega) was used to assess cell viability.

Plasmid Construction The full-length wild-type (WT) CDK12 (GenBank No. 51755) and the Ser423Ala (S423A), Ser1083Ala (S1083A), and Ser423Ala/Ser1083Ala (S423A/S1083A) mutant forms of CDK12 were subcloned into the pcDNA3.1(+) (Invitrogen).

Immunoprecipitation Cell pellets were suspended in lysis buffer (50 mM Tris-HCl pH 7.5, 150 mM NaCl, 0.5% NP-40, 5% Glycerol). After sonication and centrifugation, the supernatant was used as cell extract. Dynabeads Protein G (Invitrogen) conjugated with antibodies against CDK12 (#26816-1-AP; Proteintech) was used. The beads were washed followed by the addition of lysate and rotational incubation for 6 h at 4°C. Samples were washed and eluted with SDS buffer.

Western Blotting (WB) Cell lysates were prepared for WB analysis as described previously.[6] Cell lysates were electrophoresed and transferred onto nitrocellulose membranes. The membranes were incubated with antibodies against RNA polymerase II (#MMS-126R-500, Convance), phospho-RNA polymerase II Ser2 (#04-1571, Millipore), phospho-RNA polymerase II Ser5 (#04-1572, Millipore), phospho-RNA polymerase II Ser7 (#04-1570, Millipore), β-actin (#5145, Cell Signaling Technology), DDB1 (#5428, Cell Signaling Technology), and FLAG (A-8592, Sigma-Aldrich). The membranes were then incubated with horseradish peroxidase-conjugated secondary antibodies (#7074, #7076, or #7077, Cell Signaling Technology). The signals were detected using ImmunoStar LD (#290-69904, FUJIFILM Wako) or ImmunoStar Zeta (#295-72404, FUJIFILM Wako). All blots were imaged using the Amersham Imager 800 (Cytiva) and quantified using ImageQuant™ TL 8.2 (Cytiva).

Purification of Recombinant CDK12 and Cyclin K Proteins and Autophosphorylation Reaction of CDK12 using γ($^{18}O_4$)-ATP Purification was conducted as previously described,[5] and the autophosphorylation reaction was performed as described in 7).

LC-MS/MS Analysis The extracted peptides were dissolved in 0.1% TFA with 2% MeCN and analyzed using an Easy nLC1000 System coupled to a Fusion Orbitrap mass spectrometer. The peptides were loaded onto a trap column (C18 Pepmap100, 3 μm, 0.075 × 20 mm) and separated on an analytical column (Reprosil-Pur C18AQ, 3 μm, 0.075 × 150 mm) at a flow rate of 300 nL/min over 45 min. The mass spectra were obtained under a data dependent mode, in which precursor spectra were acquired in the Orbitrap mass analyzer at a resolution of 120,000 at m/z 200 and product ion spectra in the ion trap by higher-energy collisional dissociation with normalized collision energy of 30%.[7]

CHX Chase Assay Herein, 293 cells were transfected with CDK12 wild-type and mutant plasmids. Four days post-transfection, CHX (100 μg/mL) was added, and cells were collected at 0, 8, 16, and 24 h. The cells were lysed, and the extracted proteins were subjected to WB analysis to quantify the band intensity of FLAG-tagged proteins at each time point. These data were then applied to statistical analysis by the Dunnett test using GraphPad Prism to evaluate the stability of CDK12.

RESULTS

Identification of Autophosphorylation Sites on CDK12 Protein To identify autophosphorylation sites, recombinant CDK12 with Cyclin K was purified to high purity. The purified proteins were incubated with γ($^{18}O_4$)-ATP, and liquid chromatography–mass spectrometry (LC-MS) analysis was conducted to detect the incorporation of ^{18}O-P into the CDK12 protein by monitoring a 6 Da shift in MS (Fig. 1A). The detected phosphorylated amino acid residues on purified CDK12 protein are shown in Fig. 1D. The exact determination of some phosphorylation sites, such as Ser255, Ser256, and Ser257, was challenging due to the inclusion of multiple serine residues in one digested peptide (Fig. 1D, Recombinant CDK12). Next, to confirm the cellular phosphorylation status and the dependency on CDK12 kinase activity, a novel and highly selective CDK12 inhibitor (CDK12i)[8] was utilized (Fig. 1B and 1C). Following treatment with CDK12i in A2780 cells, cell extracts were subjected to phosphoproteomic analysis. Among the identified phosphorylated residues in purified CDK12 protein, Ser423 and Ser1083 showed a 0.6- and 0.4-fold decrease, respectively, thereby indicating that these residues are phosphorylated in a manner dependent on CDK12 kinase activity in cells (Fig. 1D, Cellular CDK12). Importantly, these residues are conserved among several species (Fig. 1E). Three-dimensional structure modeling provided by AlphaFold showed that these residues are located in disordered regions rather than the kinase domain (Fig. 1F). Collectively, we successfully identified autophosphorylation sites of the CDK12 protein (Supplemental Fig. 1).

Impact of Phosphorylation at Ser423 on CDK12 Protein Stability Since the Ser423 and Ser1083 on CDK12 were identified as autophosphorylation sites (Fig. 1D), we assessed the half-life of wild type-CDK12 (WT), mutants with Ser423 replaced by Alanine (S423A), Ser1083 replaced by Alanine (S1083A), and both (S423A/S1083A) by cycloheximide treatment to investigate the impact of these phosphorylation on CDK12. As shown in Fig. 2A and 2B, the half-life of CDK12 S423A and S423A/S1083A was shortened compared to WT or S1083A, indicating that phosphorylation at S423 plays a role in maintaining CDK12 protein stability. To clarify the mechanism of stabilization by phosphorylation on Ser423, we evaluated the association of CDK12 with DDB1, known as a regulator of CDK12 degradation; however, no change in the interaction between DDB1 and CDK12 was observed (Fig. 2C, Supplemental Fig. 2). Additionally, the localization of these CDK12 mutants was not altered (Supplemental Fig. 3).

A)

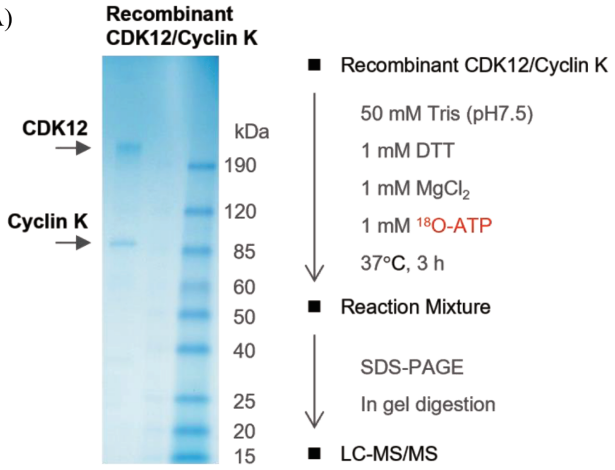

B)

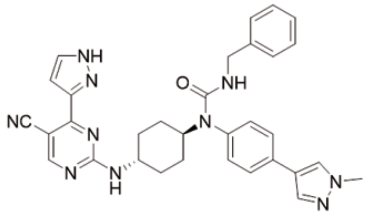

C)

Kinase	IC_{50} value (nM)
CDK12	9.6
CDK2	1500
CDK7	>4000
CDK8	>4000
CDK9	480

D)

Detected Peptide Sequence of CDK12	Recombinant CDK12			Cellular CDK12		
	Phos-site	Phosphorylated ratio (%)		Phos-site	Ratio to DMSO	
		^{16}O-P	^{18}O-P		DMSO	CDK12i
QDDSPSGASYGQDYDLSPSR	S249	100	–	S249	1	2.4
				S236 and S249	1	1.0
SHTSSNYDSYK	T255 or S256 or S257	34	66	T255 or S256 or S257	–	–
QSVSPPYKEPSAYQSSTR	S274 or S276	93	7	S274 and S276	1	1.0
QRSVSPYSR	S301 and S303	100	–	S301 and S303	1	1.0
SSSPFLSK	S334	17	83	S332 and S334	1	0.9
				S334	1	1.2
SLSRSPLPSR	S343 and S345	57	43	S343 and S345	1	1.4
HSSISPVRLPLNSSLGAELSR	S382 or S383, and S385	100	–	S383 and S385	1	1.0
GSPVFLPR	S423	35	65	S423	1	0.6
KENSSVEAKDSGLESK	S440	5	95	–	–	–
EEIVTPK	T514	26	74	–	–	–
HLLTDLPLPPELPGGDLSPPDSPEPK	S681 or S685	100	–	S681 and S685	1	1.0
AITPPQQPYK	T692	93	7	T692	1	0.9
LYNSEESRPYTNK	T893	100	–	T893	1	0.9
QRQSGVVVEEPPPSK	S1053	21	79	–	–	–
QSGVVVEEPPPSKTSR	S1063	1	99	–	–	–
QSGVVVEEPPPSKTSR	S1065	1	99	–	–	–
NSSPAPPQPAPGK	S1083	61	39	S1083	1	0.4
EAPSAPVILPSAEQTTLEASSTPADQNILAVLLSQLMK	S1200 or S1201 or T1202	97	3	–	–	–
TPTMPQEEAAAPPHILPPEK	T1246	100	–	–	–	–

Autophospholylation-site

E)

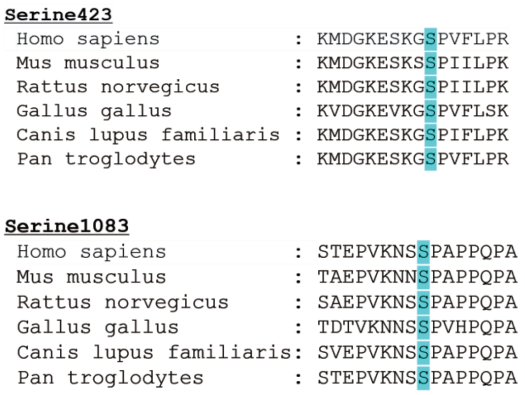

F)

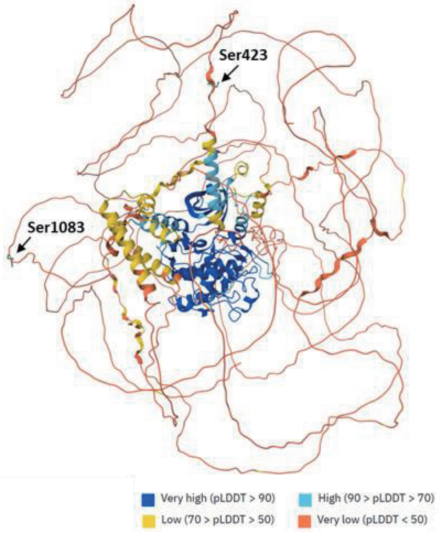

Fig. 1. Identification of Autophosphorylation Sites on CDK12

(A) Left: Coomassie Brilliant Blue (CBB) staining of purified CDK12 protein with Cyclin K. Right: Experimental procedure for identifying autophosphorylated amino acids of purified proteins using LC-MS/MS. (B) Chemical structure of CDK12i, a novel compound that selectively inhibits CDK12. (C) Enzymatic kinase selectivity of CDK12i over CDK12, CDK2, CDK7, CDK8, and CDK9 recombinant proteins. IC_{50} values for each kinase are shown. (D) Summary of the identified phosphorylated amino acids from the experiments in (A) and the identified phosphorylated sites of cellular CDK12 following treatment with CDK12i inhibitor in A2780 cell lysate by LC-MS analysis. The detected peptide sequence, start and end amino acid numbers, and phosphorylation sites are shown. For recombinant CDK12, the basal ratio of phosphate is calculated using the formula ^{16}O-P/total detected phosphorylated peptide (^{16}O-P + ^{18}O-P). Additional uptake is calculated using the formula ^{18}O-P/total detected phosphorylated peptide (^{16}O-P + ^{18}O-P). ND: peptide was not detected in this assay. (E) Alignment of the one-dimensional sequence surrounding Ser423 and Ser1083 among several species. (F) AlphaFold-based structural modeling and representation of two amino acids: Ser423 and Ser1083.

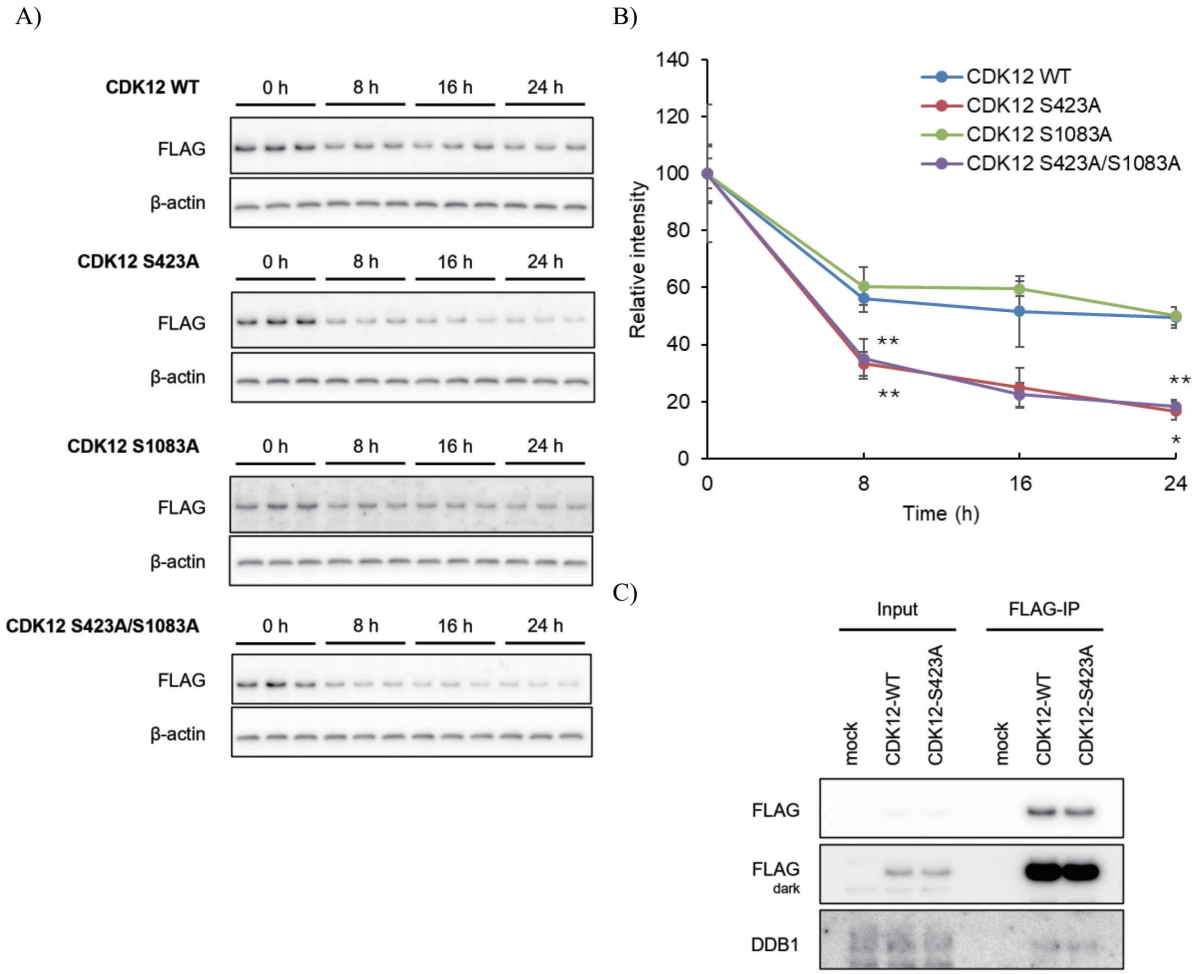

Fig. 2. Impact of Phosphorylation at Ser423 on CDK12 Protein Stability

(A) Half-life analysis by cycloheximide chase, monitoring the expression of exogenous CDK12-wild type (WT), S423A mutant, S1083A mutant, and S423A/S1083A double mutant. (B) Quantitative analysis of the results in (A). (C) Interaction between CDK12 and DDB1. Overexpressed CDK12-WT and S423A mutant were immunoprecipitated and subjected to WB by indicated antibodies.

CDK7- or CDK9-mediated Phosphorylation of CDK12 at Ser423 and Other Autophosphorylation Sites Most of the identified autophosphorylation sites on the CDK12 protein were located within consensus sequences targeted by CDKs, which include serine or threonine at the -1 position of proline.[3,9,10] This suggested that CDK7 or CDK9 might also phosphorylate these residues on CDK12. To clarify the functional interconnection among transcriptional CDK7 and CDK9 (Fig. 3A), a comprehensive phosphoproteomic analysis focusing on the CDK12 protein was conducted. Prior to the experiment, we determined the appropriate concentrations for each inhibitor: the CDK7 inhibitor CT7001 (Samuraciclib) and CDK9 inhibitor BAY-1251152 (Enitociclib) effectively inhibited their respective targets, Ser5 or Ser2 of Pol II (Fig. 3B) and confirmed anti-growth activity (Fig. 3C). Based on these results, we concluded that optimal inhibition of CDK7 or CDK9 occurs at 3 μM for CT7001 and 1 μM for BAY-1251152 in cells. Following immunoprecipitation and MS analysis of endogenous CDK12 proteins treated with these inhibitors for 6 h, the phosphorylation levels of detected residues on CDK12 were assessed (Fig. 3D). As shown in Fig. 3E, ten phosphorylated peptides were detected, several of which decreased following CDK7 or CDK9 inhibitor treatment. Notably, the autophosphorylation at Ser423 on cellular CDK12 was affected by CT7001 (64%), but was largely unaffected by BAY-1251152 (107%). Additionally, Thr514, identified in recombinant CDK12, was inhibited by both CT7001 and BAY-1251152 (20% or 49% relative to DMSO, respectively). Although the biological significance of phosphorylation at Thr514 of CDK12 remains unclear, these data indicate that CDK7 and CDK9 modulate CDK12 by influencing its autophosphorylation and other phosphorylation sites on the CDK12 protein (Fig. 3F).

Comprehensive Analysis of the Interactome Between CDK12 and Phosphorylated Proteins Following Treatment with CDK7 or CDK9 Inhibitors In Fig. 3, we demonstrated the different effect of CDK7 and CDK9 on several phosphorylation of CDK12 were demonstrated. Next, we conducted a comprehensive interactome analysis between CDK12 and phosphorylated proteins by CDK12 following treatment with CDK7 or CDK9 inhibitors under the same experimental conditions as Fig. 3D. As a result, we identified 29 down-regulated (log2 fold change < -0.5 and Q-value < 0.3) and 19 up-regulated (log2 fold change > 0.5 and Q-value < 0.3) phosphorylation sites following 6 h of treatment with CT7001 at 3 μM (Fig. 4A). Additionally, we identified 26 down-regulated and 36 up-regulated phosphorylation sites following 6 h of treatment with BAY-1251152 at 1 μM (Fig. 4B).

A)

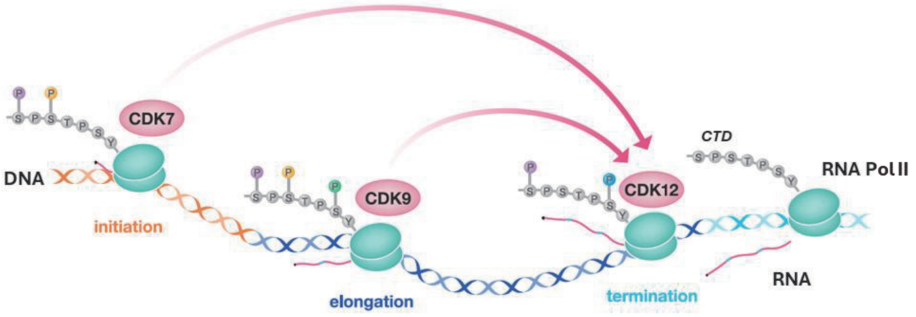

B)

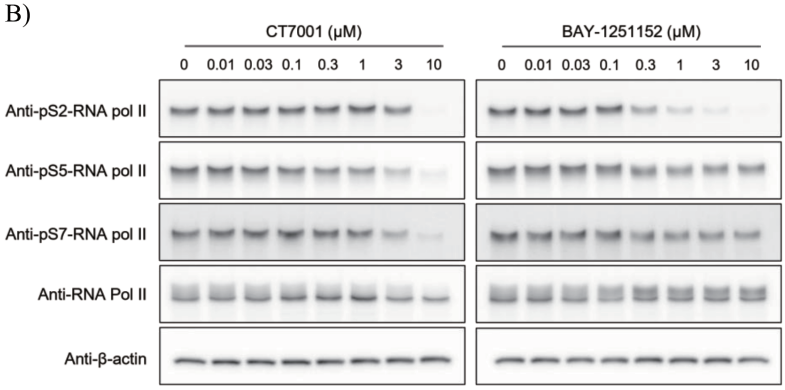

C)

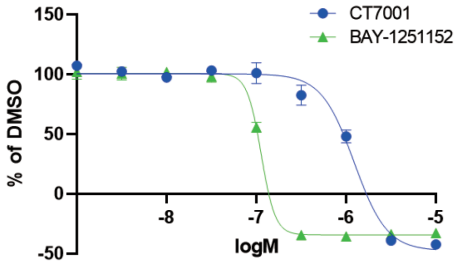

D)

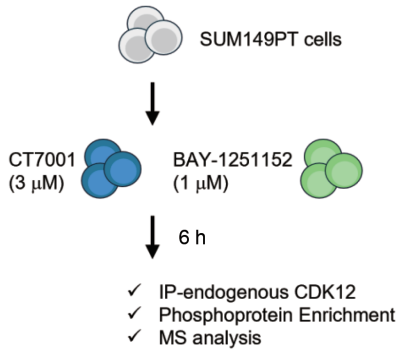

E)

Target		CDK7i		CDK9i	
Compounds		CT7001 (3 μM)		BAY-1251152 (1 μM)	
Protein	Phos-site	% of DMSO	P-value	% of DMSO	P-value
CDK12	S274, S276	14%	0.22	31%	0.31
	S334	44%	0.33	53%	0.47
	S383, S385	94%	0.73	91%	0.42
	S423	64%	0.02	107%	0.46
	T514	20%	0.00	49%	0.17
	S681	97%	0.97	74%	0.61
	T692	82%	0.18	80%	0.15
	T893	57%	0.26	96%	0.46
	S1083	87%	0.43	81%	0.30
	T1246	81%	0.77	84%	0.82

Autophospholylation-site

F)

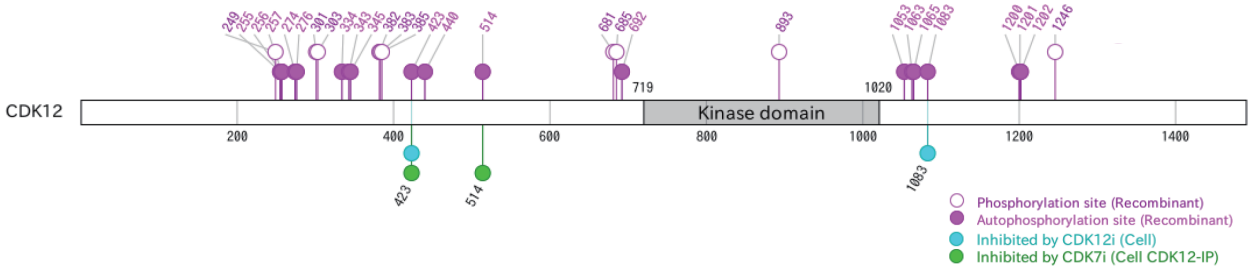

Fig. 3. CDK7- or CDK9-mediated Phosphorylation of CDK12 at Ser423 and Other Autophosphorylation Sites

(A) Concept of this research: elucidation of the interconnection among CDK7, CDK9, and CDK12. Previous studies have reported CDK7-mediated phosphorylation of CDK9 and CDK12.[3)] (B) Dose-response analysis of CDK7 inhibitor (CDK7i), CT7001 and CDK9 inhibitor (CDK9i), BAY-1251152 in SUM149PT cells. After 8 h of treatment, WB was conducted using the indicated antibodies. (C) In vitro growth assay of SUM149PT cells treated with CT7001 and BAY-1251152 for 72 h. Cell viability was measured using CellTiter-Glo, and the percentage of survival (% of DMSO) was calculated to assess growth inhibition (adjusted to day 0 for all points). (D) Experimental procedure for (E): Following treatment with CT7001 and BAY-1251152 for 6 h, endogenous CDK12 was immunoprecipitated and further purified using titanium beads to concentrate phosphopeptides. The samples were then subjected to LC-MS analysis. (E) The fold change in phosphorylation at each amino acid under CDK7i or CDK9i treatment conditions was calculated relative to the untreated condition (DMSO). (F) Summary of the identified phosphorylated amino acids on CDK12. Upper circle flags indicate the phosphorylation sites identified in purified protein and cell-based experiments (Fig. 1D), while the lower circle flags indicate the phosphorylation sites identified after treatment with CDK12 inhibitor (CDK12i) and CDK7i, as shown in Fig. 1D and 3E, respectively.

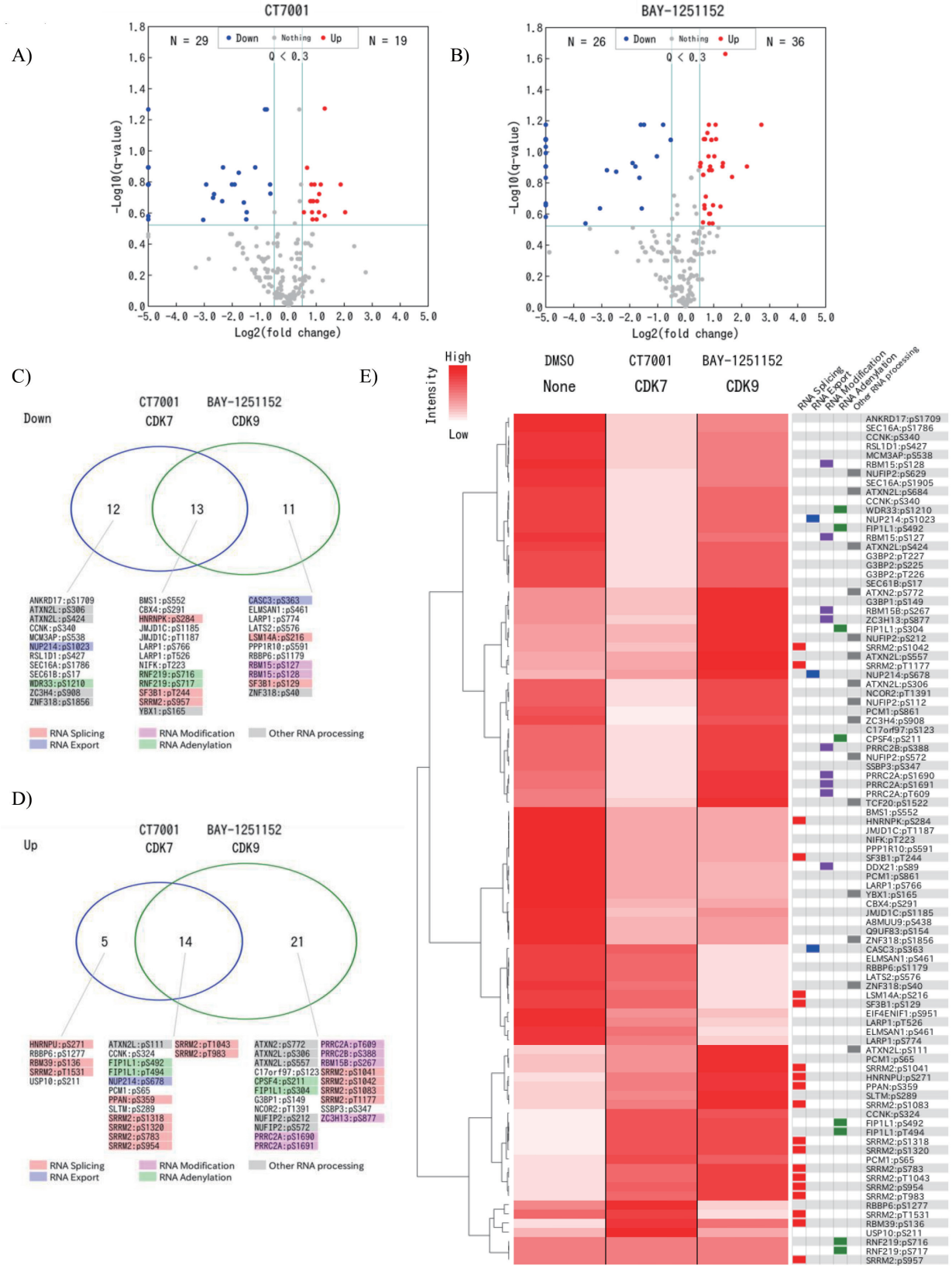

Fig. 4. Comprehensive Analysis of the Interactome Between CDK12 and Phosphorylated Proteins Following Treatment with CDK7 or CDK9 Inhibitors

(A, B) Log2(fold change) volcano plots of differentially phosphorylated sites in A2780 cells treated with CT7001 (A) or BAY-1251152 (B) for 6 h, relative to dimethyl sulfoxide (DMSO) treatment. Highlighted points represent phosphorylation sites with a Q-value of <0.3 and Log2(fold change) > 0.5 compared to DMSO treatment. The numbers of up-regulated and down-regulated sites are indicated. (C, D) Venn diagrams showing the overlap of down-regulated phosphorylation sites (C) or up-regulated phosphorylation sites (D) following treatment with CDK7 inhibitor CT7001 or CDK9 inhibitor BAY-1251152, in comparison with the 42 immunoprecipitated CDK12 phosphorylation sites. (E) Heatmap analysis of the down-regulated and up-regulated CDK12 phosphorylation sites following treatment with CT7001 or BAY-1251152 based on the average of triplicate data.

In the down-regulated (Fig. 4C) and up-regulated (Fig. 4D) proteins, some phosphorylation amino acid residues were shared in both CDK7 and CDK9 inhibitor treatment, while several independent sites were also detected. This result is consistent with their various effects on the phosphorylation sites of CDK12 (Fig. 3E). Indeed, viewing the overall heat map, CT7001 suppressed phosphorylation of the RNA modulation proteins, which are concentrated at upper part of the heat map (Fig. 4E, purple), while BAY-1251152 increased or weakly repressed them. This observation supports the distinct effects of CDK7 and CDK9 on the CDK12 interactome. Interestingly, a common action of CDK7 and CDK9 inhibitors was to enhance the phosphorylation of the splicing factors SRRM2, PPAN, HNRNPU and RBM39, which are concentrated at the bottom of the heatmap (Fig. 4E, red).

DISCUSSION

The interconnection among transcriptional processes has been proposed, yet understanding this connection in the context of mRNA transcription remains underexplored. Previous studies have identified CDK7-mediated phosphorylation of CDK12 and discussed overlapping substrates among CDK7, CDK9, and CDK12.[3,8-10] However, the regulation of CDK12 by other transcription-associated kinases, such as CDK7 and CDK9, is not fully understood. Beyond its fundamental role in mRNA synthesis, research on CDK12 has gained momentum due to the development of novel therapeutic agents targeting this kinase.

In this study, we first identified the autophosphorylation sites of CDK12 (Fig. 1D). While previous reports suggested CDK12 autophosphorylation, the specific amino acids had not been analyzed.[11] We identified and validated numerous phosphorylation sites, which were located not only in the T-loop but also in disordered regions (Supplemental Fig. 2A). However, not all phosphorylation sites identified in the recombinant CDK12 protein were confirmed in cells (Fig. 1C); this is possibly due to slow turnover influenced by phosphatase activity in cell. Although Protein Phosphatase 1 Binding Protein (PPP1R10) was identified as an interacting protein (Fig. 4E), the specific phosphatases for CDK12 remain unidentified. Determining these phosphatases might provide further insights into the regulation of CDK12.[12,13] Interestingly, several sites including Ser249, Ser334, and Ser343/345 showed increased phosphorylation following CDK12i treatment (Fig. 1D), thereby indicating a compensatory mechanism supporting transcriptional activity under CDK12 inhibition might exist. Among these, the feedback response to Ser334 tended to be a target of CDK7 and CDK9, although other transcription-associated kinases may also be involved (Fig. 3E).[14]

Secondly, the half-life of CDK12 was shortened by disrupting Ser423 phosphorylation, and the exact function of this phosphorylation remains unclear despite being identified as an autophosphorylation site. Known factors affecting CDK12 protein stabilization are limited, with the DDB1-CUL4-RBX1 E3 ubiquitin ligase being one known factor.[15] However, our experiments did not show differences in interaction with DDB1, thereby suggesting other factors might affect stability via Ser423 phosphorylation (Fig. 2C). Since E3 ligase RBBP6 and SUMO ligase CBX4 were identified as interacting proteins with CDK12 and they were also targets of CDK7 or CDK9 (Fig. 4E), their interaction status might affect the half-life of the CDK12 protein. At least, Ser423 appears to be a crucial point for CDK12 stability regulated by autophosphorylation and CDK7-mediated modifications. The unique post-translational modification of Ser423, which is not conserved between CDK12 and CDK13, indicates a specific regulatory mechanism for CDK12.[16]

Most importantly, as shown in Fig. 3E, a crosstalk among CDK7, CDK9, and CDK12 in terms of phosphorylation on CDK12 could be proposed. Additionally, the interactome of CDK12 with phosphorylated proteins displayed distinct patterns of disruption and stimulation between CDK7 and CDK9 inhibition. Although some aspects remain unclear, it was suggested that CDK12 is coordinately activated by CDK7 and CDK9, respectively.

In summary, through comprehensive analysis focusing on CDK12 phosphorylation, we suggest a significant interconnection among transcriptional processes. Recent studies have shown that the abnormal activity of these CDKs contributes to the proliferation and survival of cancer cells, thereby leading to advancements in the development of cancer therapies targeting each transcriptional CDKs. Further analysis will illuminate the details of the relationship among these CDKs, which will be useful in the development of new drugs targeting them.

Acknowledgments We are grateful to Professor Kosuke Yusa from Kyoto University for their valuable discussions.

Conflict of interest HY, SE, MY, KS, and DM are employees of Chordia Therapeutics, Inc. KH and SA are employees of Axcelead Drug Discovery Partners, Inc. and Takeda Pharmaceutical Co., Ltd, respectively.

Supplementary Data Supplementary data for this article can be found online.

REFERENCES

1) Vervoort SJ, Devlin JR, Kwiatkowski N, Teng M, Gray NS, Johnstone RW. Targeting transcription cycles in cancer. *Nat. Rev. Cancer*, **22**, 5–2 (2022).
2) Harlen KM, Churchman LS. The code and beyond: transcription regulation by the RNA polymerase II carboxy-terminal domain. *Nat. Rev. Mol. Cell Biol.*, **18**, 263–273 (2017).
3) Rimel JK, Poss ZC, Erickson B, Maas ZL, Ebmeier CC, Johnson JL, Decker TM, Yaron TM, Bradley MJ, Hamman KB, Hu S, Malojcic G, Marineau JJ, White PW, Brault M, Tao L, DeRoy P, Clavette C, Nayak S, Damon LJ, Kaltheuner IH, Bunch H, Cantley LC, Geyer M, Iwasa J, Dowell RD, Bentley DL, Old WM, Taatjes DJ. Selective inhibition of CDK7 reveals high-confidence targets and new models for TFIIH function in transcription. *Genes Dev.*, **34**, 1452–1473 (2020).
4) Bartkowiak B, Yan CM, Soderblom EJ, Greenleaf AL. CDK12 activity-dependent phosphorylation events in human cells. *Biomolecules*, **9**, 634 (2019).
5) Ito M, Tanaka T, Toita A, Uchiyama N, Kokubo H, Morishita N, Klein MG, Zou H, Murakami M, Kondo M, Sameshima T, Araki S, Endo S, Kawamoto T, Morin GB, Aparicio SA, Nakanishi A, Maezaki H, Imaeda Y. Discovery of 3-Benzyl-1-(trans-4-((5-cyanopyridin-2-yl) aminocyclohexyl)-1-arylurea Derivatives as Novel and Selective Cyclin-Dependent Kinase 12 (CDK12) Inhibitors. *J. Med. Chem.*, **61**, 7710–7728 (2018). Epub Aug 20, 2018.
6) Morishita D, Katayama R, Sekimizu K, Tsuruo T, Fujita N. Pim kinases promote cell cycle progression by phosphorylating and down-regulating p27Kip1 at the transcriptional and posttranscriptional levels. *Cancer Res.*, **68**, 5076–5085 (2008).
7) Iwai K, Yaguchi M, Nishimura K, Yamamoto Y, Tamura T, Nakata D, Dairiki R, Kawakita Y, Mizojiri R, Ito Y, Asano M, Maezaki H,

Nakayama Y, Kaishima M, Hayashi K, Teratani M, Miyakawa S, Iwatani M, Miyamoto M, Klein MG, Lane W, Snell G, Tjhen R, He X, Pulukuri S, Nomura T. Anti-tumor efficacy of a novel CLK inhibitor via targeting RNA splicing and MYC-dependent vulnerability. *EMBO Mol. Med.*, **10**, e8289 (2018).
8) WO/2019/189555 Heterocyclic Compound.
9) Decker TM, Forné I, Straub T, Elsaman H, Ma G, Shah N, Imhof A, Eick D. Analog-sensitive cell line identifies cellular substrates of CDK9. *Oncotarget*, **10**, 6934–6943 (2019).
10) Sansó M, Levin RS, Lipp JJ, Wang VY, Greifenberg AK, Quezada EM, Ali A, Ghosh A, Larochelle S, Rana TM, Geyer M, Tong L, Shokat KM, Fisher RP. P-TEFb regulation of transcription termination factor Xrn2 revealed by a chemical genetic screen for Cdk9 substrates. *Genes Dev.*, **30**, 117–131 (2016).
11) Liang K, Gao X, Gilmore JM, Florens L, Washburn MP, Smith E, Shilatifard A. Characterization of human cyclin-dependent kinase 12 (CDK12) and CDK13 complexes in C-terminal domain phosphorylation, gene transcription, and RNA processing. *Mol. Cell. Biol.*, **35**, 928–938 (2015).
12) Bartkowiak B, Greenleaf AL. Expression, purification, and identification of associated proteins of the full-length hCDK12/CyclinK complex. *J. Biol. Chem.*, **290**, 1786–1795 (2015).
13) Dubbury SJ, Boutz PL, Sharp PA. CDK12 regulates DNA repair genes by suppressing intronic polyadenylation. *Nature*, **564**, 141–145 (2018).
14) Cossa G, Parua PK, Eilers M, Fisher RP. Protein phosphatases in the RNAPII transcription cycle: erasers, sculptors, gatekeepers, and potential drug targets. *Genes Dev.*, **35**, 658–676 (2021).
15) Słabicki M, Kozicka Z, Petzold G, Li YD, Manojkumar M, Bunker RD, Donovan KA, Sievers QL, Koeppel J, Suchyta D, Sperling AS, Fink EC, Gasser JA, Wang LR, Corsello SM, Sellar RS, Jan M, Gillingham D, Scholl C, Fröhling S, Golub TR, Fischer ES, Thomä NH, Ebert BL. The CDK inhibitor CR8 acts as a molecular glue degrader that depletes cyclin K. *Nature*, **585**, 293–297 (2020).
16) Chou J, Quigley DA, Robinson TM, Feng FY, Ashworth A. Transcription-associated cyclin-dependent kinases as targets and biomarkers for cancer therapy. *Cancer Discov.*, **10**, 351–370 (2020).